Journal of Alloys and Compounds 495 (2010) 305–308

Contents lists available at ScienceDirect

Journal of Alloys and Compounds

journal homepage: www.elsevier.com/locate/jallcom

AgGeSe-based bulk glasses: A survey of their fundamental properties

M.A. Ureña [a], M. Fontana [a], A. Piarristeguy [b], B. Arcondo [a,*]

[a] Laboratorio de Sólidos Amorfos, Facultad de Ingeniería, INTECIN, UBA-CONICET, Paseo Colón 850, C1063ACV Buenos Aires, Argentina
[b] PMDP, Institut Charles Gerhardt, Montpellier (UMR 5253 CNRS), Univ. Montpellier 2, Place Eugène Bataillon, 34095 Montpellier, France

ARTICLE INFO

Article history:
Received 17 September 2008
Received in revised form 29 October 2009
Accepted 13 November 2009
Available online 22 December 2009

Keywords:
Amorphous materials
Liquid quenching
Scanning electron microscopy
Ionic conduction

ABSTRACT

Ge_xSe_{1-x} system is a well-known glass former for $x \leq 0.43$. The addition of third elements (i.e. Ag, Sb, and Sn) even up to high concentrations is possible without affecting its glass forming ability. These metals confer these glasses very particular properties. Ag–Ge–Se glasses are semiconductors for low Ag concentration whereas they are fast ionic conductors above 8 at.% Ag. The structure, thermal behaviour and transport properties of these glasses are analyzed.

Metal doping is easily performed in chalcogenide glasses. It has been observed that, in contrast to crystalline semiconductors, their transport properties were not substantially affected as the valence bonds of the doping elements are completely saturated. The resource of doping with a ^{57}Fe probe is widely employed in the materials study in order to characterize the short-range order of their structure by means of Mössbauer effect spectroscopy.

These results are discussed and correlated to the structure and morphology of this chalcogenide system.

1. Introduction

Ag–Ge–Se equilibrium phase diagram [1] is dominated by liquid immiscibility. The pseudobinary section Ag_2Se–$GeSe_2$ that divides the diagram (Fig. 1) presents two eutectic transformations: e_2 formed by Ag_2Se and γAg_8GeSe_6 (τ) at 810 °C and e_1 formed by τ and $GeSe_2$ at 560 °C. The section τ–Se is pseudobinary with a monotectic reaction $L_1 \Leftrightarrow \tau + L_2$ at 700 °C and a eutectic reaction $L \Leftrightarrow \tau + Se$ at 220 °C. In the partial ternary system Ag_2Se–τ–Se there is a ternary monotectic reaction $L_5 \Leftrightarrow L_6 + \tau + Ag_2Se$ at 615 °C followed by a ternary eutectic reaction near the Se corner whereas the Se 66.67 at.% section presents a 400 °C invariant attributed to the monotectic reaction $L_7 \Leftrightarrow L_8 + \tau + GeSe_2$.

The aim of this work is to analyze the morphology of bulk glasses of the subsystem τ–Se–$GeSe_2$ obtained by melt quenching and to correlate their fundamental properties with glasses morphology. Structural characterization, thermal behavior and electric transport properties are reviewed departing from previous work of the authors.

2. Experimental procedure

$Ag_y(Ge_xSe_{1-x})_{100-y}$ glasses with $x = 0.20$ and 0.25 and $y = 0$, 5, 10, 20, and 25 at.% were obtained by the joint melting of the elemental constituents (5 N purity) in previously evacuated (10^{-6} mbar) and sealed quartz ampoules. After 8 h at 910 °C the ampoules containing the liquid samples were quenched in an ice–water mixture. Other set of samples of composition $Ag_y(Ge_{0.25}Se_{0.75})_{100-y}$ with $y = 0$, 5, 10 and 25 at.% doped with 0.5% Fe were obtained with the same procedure. In this case the isotopic composition of Fe was enriched with ^{57}Fe isotope to a 90%.

Morphology characterization of these glasses was performed in a scanning electron microscope Philips XL 30CP with a back scattering electron detector employing an acceleration voltage of 25 kV. Structure has been studied by X-ray diffractometry (XRD) using a (–(diffractometer with monochromatised Mo(Kα) radiation. A Zr filter was used to eliminate the fluorescence radiation. XRD patterns were obtained in the wave number range $0.5\ Å^{-1} < q < 10\ Å^{-1}$ ($q = (4\pi/\lambda)\sin\theta$). The statistical error is about 1% in the range $0.5\ Å^{-1} < q < 5\ Å^{-1}$ and 1.5% in the range $5\ Å^{-1} < q < 10\ Å^{-1}$. XRD patterns were analyzed as is reported in [2]. Thermal analysis was performed in a differential scanning calorimeter (DSC) PerkinElmer DSC-7 under dynamic Ar. Bulk samples were milled to have a uniform grain size ranging between 25 and 50 μm. All powder samples weighted 5.00 ± 0.05 mg and were sealed in aluminium pans. The experimental data was analyzed as is described in [3]. Electrical measurements were done by using the impedance spectroscopy technique in the frequency range from 5 Hz to 2 MHz at the temperature range 293–363 K (below the glass temperature of the samples, $T_g > 497$ K). The measurement cells were made as is described in [4]. DC measurements were also performed to characterize whether conduction was ionic or electronic.

Samples containing Fe were additionally analyzed by means of Mössbauer spectroscopy in transmission geometry employing a ^{57}Fe(Rh) source with constant acceleration. Measurements were carried out on samples at room and lower temperatures (300 K, 195 K and 77 K) as is described in [5].

3. Results and discussion

3.1. Morphology

As a consequence of the liquid miscibility gap, bulk glasses with $x = 0.20$, 0.25 at. fraction and $5 < y < 25$ at.% are inhomoge-

* Corresponding author. Tel.: +54 11 43429184; fax: +54 11 43311852.
E-mail address: barcond@fi.uba.ar (B. Arcondo).

0925-8388/$ – see front matter © 2009 Elsevier B.V. All rights reserved.
doi:10.1016/j.jallcom.2009.11.081

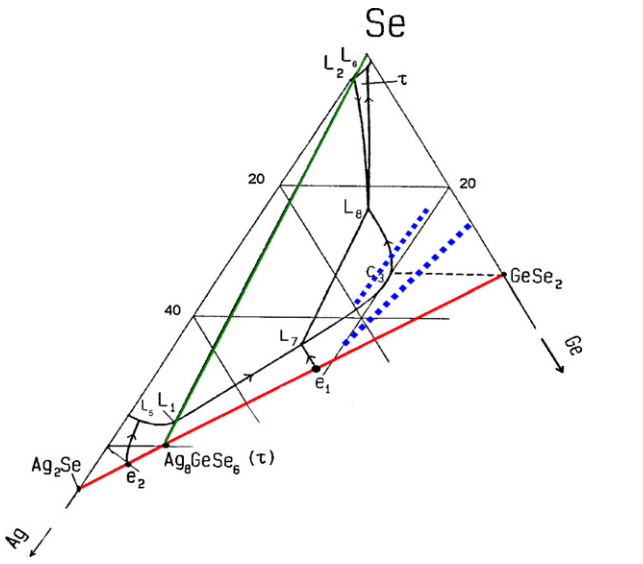

Fig. 1. Liquidus projection of the ternary system Ag_2Se–Se–$GeSe_2$. Dotted lines correspond to the composition of the obtained bulk glasses. Additional information in the text.

neous as is shown in Fig. 2 where two phases, a bright one with higher Ag content and a dark one with lower Ag concentration are present. Similar results were reported in [6,7]. In the case of samples with $5 < y < 8$ at.% the Ag-rich phase is forming dots (which size depends on composition) immersed in a dark Ag depleted matrix as a product of a binodal transition. This morphology is also present for samples with $10 < y < 25$ at.% whereas samples with $y = 25$ at.% do not follow the same trend. In that range the matrix is Ag-rich whereas the dots are Ag depleted. Between both regimes $8 \leq y \leq 10$ at.%, samples present the fingerprints of a spinodal decomposition where bright and dark zones interlace forming a bi-continuous morphology. Following Cahn [8] the connectivity of both phases is expected when the volume fraction of the minor phase exceeds about 15%. Assuming as in [5] that bright phase is similar to Ag_8GeSe_6 and dark phase is not far from Ge_tSe_{1-t}, samples with $x = 0.25$ atomic fraction may be decomposed as glassy $m(Ag_8GeSe_6) + Ge_tSe_{1-t}$ with m the number of moles of the Ag-rich phase and $t = (25 - 3m)/(100 - 15m)$, Ge atomic fraction in the dark phase. In order to estimate the molar fraction of the minor phase when the connectivity of the minor phase is attained, its density is assumed to be about 85% of the density of the crystalline compound, that is $\sim 6\,g\,cm^{-3}$, and the overall density $\delta \sim 4.8\,g\,cm^{-3}$ is obtained from [2] for Ag content $8 \leq y \leq 10$ at.%. The number of moles of the minor phase results $m \approx 1$ when connectivity is attained. Consequently the minimum Ag concentration needed for a bi-continuous morphology is about 8 at.%. However this is only a rough approximation as both phases contain Ag as has been reported in [9]. Phase separation in Ag–Ge–Se bulk glasses in the subsystem τ–Se–$GeSe_2$ has also been reported by [10,11]. These authors indirectly observed glass inhomogeneity employing different techniques. However, they report that the separated phases are a Ag_2Se-rich glass and a Ge_tSe_{1-t} backbone. As a consequence, the composition of the separated phases remains controversial.

3.2. Structure

The structure of $Ag_y(Ge_{0.25}Se_{0.75})_{100-y}$ glasses with $0 \leq y \leq 25$ at.% has been analyzed in [2]. The existence of intermediate range order (IRO) associated to a prepeak or first sharp diffraction peak (FSDP) in the structure factor $S(q)$ around $1.0\,Å^{-1}$ is observed [2]. The FSDP position of the ternary glasses is slightly

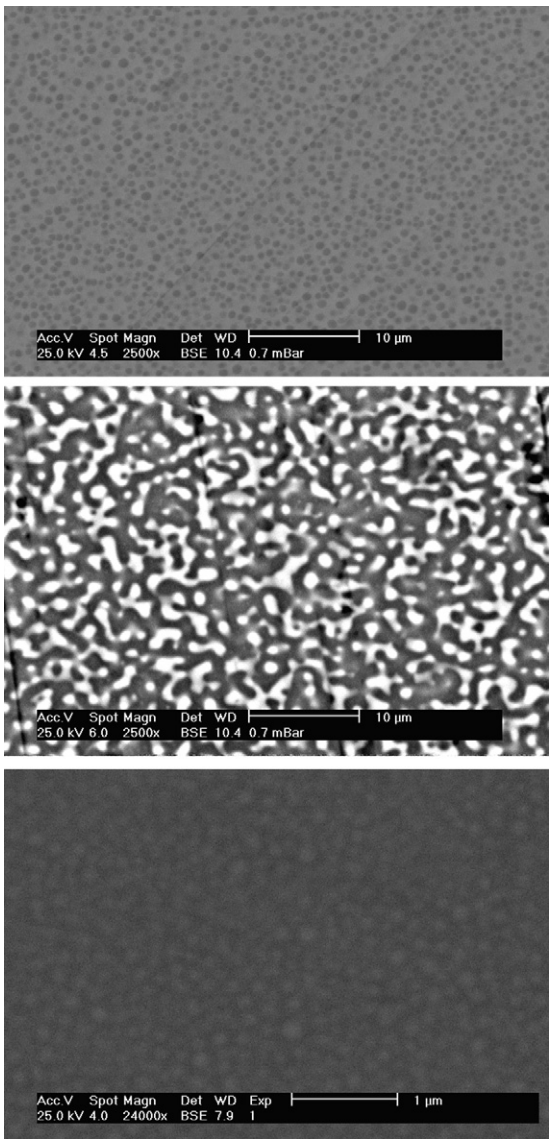

Fig. 2. Scanning electron micrographs, obtained with back scattering electron detector, of bulk glasses which compositions are: from top to bottom $Ag_{20}(Ge_{0.25}Se_{0.75})_{80}$, $Ag_{10}(Ge_{0.25}Se_{0.75})_{90}$ and $Ag_7(Ge_{0.25}Se_{0.75})_{93}$.

bigger than that of the binary glass and its area decreases due to a change of the IRO upon adding Ag. According to morphology results changes in the FSDP position may be attributed to variations of the composition of both phases with the overall composition of the glass whereas IRO lowering may be attributed to the increasing of Ag-rich volume fraction at the expenses of Ag depleted zones characterized by a strong IRO.

3.3. Thermal behavior

The thermal behavior of $Ag_y(Ge_{0.25}Se_{0.75})_{100-y}$ glasses with $y = 10$, 15, 20, and 25 at.% has been exhaustively analyzed in [3]. A glass transition was observed for all samples at about 505 K (for a heating rate $\beta = 10\,K\,min^{-1}$). A first crystallization peak (T_1), corresponding to τ phase, is observed for all samples and all heating rates. For $\beta = 10\,K\,min^{-1}$, T_1 is in the range 579.1–595.0 ± 0.5 K (T_1 increases as Ag concentration grows). The fact that the first crystallization product is τ phase is in agreement with the assumption that Ag-rich phase composition is not far from Ag_8GeSe_6. A second crystallization peak (T_2) in the range 652.4–672.5 ± 0.5 K (T_2

lowers as Ag concentration grows) corresponds to $GeSe_2$. Finally, an intermediate peak is observed, for sample with 25 at.% Ag, at 615 K. Room temperature (RT) XRD pattern of the sample heated up to this temperature shows the presence of both Ag_8GeSe_6 and $GeSe_2$. These results do not agree with those obtained with temperature modulated DSC by [10,11] who observed bimodal glass transition temperatures ($T_g^a = 503$ K and $T_g^b = 563$ K for samples $Ag_{25}(Ge_{0.25}Se_{0.75})_{75}$) that they attribute to g-Ag_2Se and Ge_tSe_{1-t} backbone, respectively. This difference can be attributed to the different techniques employed. On the other hand, our results do not completely agree with those obtained by [12,13] employing neutron thermo-diffractometry (NTD), however, most of the differences can be attributed to the different β values employed ($\beta \geq 10$ K min^{-1} in DSC whereas $\beta = 0.2$ K min^{-1} in NTD). The main differences in this case correspond to the crystallization temperatures that are lower for NTD. On the other hand, NTD patterns of $y = 25$ show the appearance of an additional unstable phase at about 570 K that decomposes above 585 K for continuous heating experiments. This unstable phase was also observed in NTD patterns obtained during isothermal treatment at 571 K [13]. The authors propose that this phase is Ag_2GeSe_3 and decomposes into $GeSe_2$ and a fourth phase $Ag_{10}Ge_3Se_{11}$. In view of this fact, the presence of $GeSe_2$ in the XRD pattern obtained at RT for sample $y = 25$ heated up to 615 K, can be attributed to the decomposition of the unstable phase in the cooling process towards RT.

The glass forming ability, GFA, of different samples is also compared in [3], the influence of melting temperature T_m, glass temperature T_g and β on the GFA is analyzed (T_m is estimated from the ternary phase diagram [1]). The GFA enhances when (a) the critical cooling rate in order to obtain the glass (β_M) decreases, or (b) $T_m - T_g$ decreases (if β is maintained constant). Therefore, one can determine which compositions (in decreasing order) have greater GFA, i.e. shorter $T_m - T_g$. The best glass former is the sample Ag25, followed in decreasing order by Ag_{10}, Ag_{15} and Ag_{20} glasses (glass samples are named Ag_y according to their Ag concentration in at.%). This trend is corroborated by the β_M values estimated from the time–temperature-transformation (TTT) diagram. On the other hand, the superposition of the glass forming range and the two-phase region is rather unusual in other ternary systems, i.e. bulk metallic glasses [14].

3.4. Electric transport

The electric transport in $Ag_y(Ge_{0.25}Se_{0.75})_{100-y}$ glasses with $0 \leq y \leq 25$ at.% has been studied in [4,15]. Two conductivity regimes are observed in agreement with [16]. Semiconductor for $y < 8$ at.% and fast ionic conductor for $y \geq 8$ at.%. The jump in conductivity (Fig. 3) can be attributed to the fact that Ag-rich bright zones isolated in a non-conducting matrix in the binodal composition range evolves towards a bi-continuous morphology in the spinodal composition range for $y \geq 8$ at.% where the Ag-rich phase connectivity gives place to fast ionic conductivity. The rough estimation of the minimum Ag concentration that grants the connectivity of the bright phase performed in 3.1 is in agreement with Ag concentration threshold for fast ionic conductivity [15]. In agreement with [17,18] $Ag_y(Ge_xSe_{1-x})_{100-y}$ glasses present, as well as other inhomogeneous glasses, an abrupt change of conductivity of several orders of magnitude.

3.5. Mössbauer effect

Mössbauer effect on Fe doped $Ag_y(Ge_{0.25}Se_{0.75})_{100-y}$ glasses has been analyzed in [5,19]. Fe doping do not impact on the glass structure of $Ag_y(Ge_{0.25}Se_{0.75})_{100-y}$ system. Amorphous samples containing 0.5% Fe do not present apparent Fe segregation.

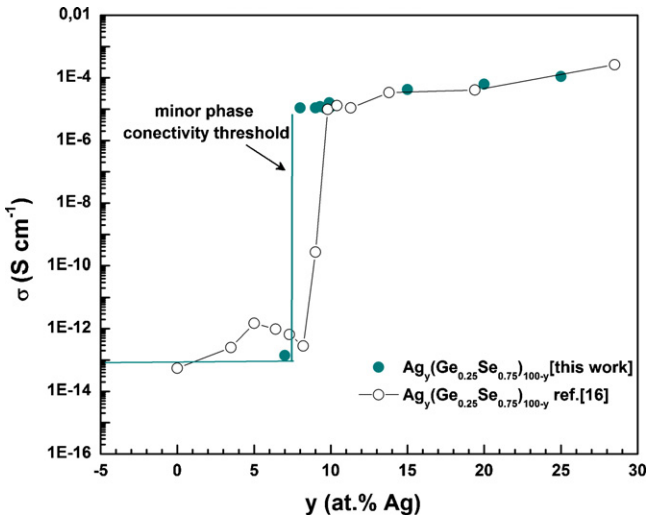

Fig. 3. Conductivity values of $Ag_y(Ge_{0.25}Se_{0.75})_{100-y}$ bulk glasses determined from complex impedance spectroscopy technique. Results reported in Ref. [16] are depicted for comparison.

Mössbauer spectra were fitted with two quadrupolar splitting (Δ) distributions corresponding to two different environments of ^{57}Fe probe. From the dependence of the recoilless fraction f on temperature (T) the Debye temperature (θ_D) of each environment is calculated.

A quadrupolar splitting distribution characterized by a large Δ doublet corresponds to high spin (HS) Fe^{2+} in distorted octahedral environments and the other characterized by a relatively small Δ corresponds to low spin (LS) Fe^{2+} in octahedral coordination. As Ag concentration increases the larger $\langle\Delta\rangle$ interaction grows.

$\theta_D = 290$ K for HS Fe^{2+} and $\theta_D = 370$ K for LS Fe^{2+} for samples with $y = 10$. The large difference in θ_D values suggests that each Fe environment (LS or HS) corresponds to a different phase. As Ag concentration increases the lower θ_D regions grow in correspondence to the increase of the bright zones area in SEM images whereas zones Ag depleted with a persistent IRO correspond to higher θ_D.

Nevertheless, for sample with $y = 25$ which present a singular morphology and GFA, $\theta_D = 316$ K for HS Fe^{2+} and $\theta_D = 270$ K for LS Fe^{2+}. However as LS Fe^{2+} area decreases more than that of HS Fe^{2+} as temperature increases, a spin switch from LS to HS states cannot be discarded and, in that case, θ_D estimations should be corrected accordingly.

4. Conclusions

$Ag_y(Ge_xSe_{1-x})_{100-y}$ glasses with Ge atomic fractions $x = 0.20$ and 0.25 and $0 \leq y \leq 25$ at.%, obtained by melt quenching, present intrinsic heterogeneity consisting of zones of different composition, basically due to Ag concentration. The heterogeneity size can be controlled with the overall composition and a small addition of Fe does not impact in these general trends.

A transition from a binodal morphology towards a morphology consisting of two interlaced phases connecting all the sample occurs for a minor phase volume fraction of about 0.15, that is Ag concentration below 10 at.%. For samples with $x = 0.25$ the concentration threshold corresponds to $y \sim 8$ at.%. As a consequence, the Ag-rich ionic conducting network connects the entire sample and a change in the electric transport behavior takes place.

Mössbauer analyses on samples with 0.5% Fe let us see that the increasing of Ag concentration as well as increases the volume of Ag-rich zones changes the bonding characteristics of both of the

phases involved. That is, as Ag concentration changes, also does the Debye temperature of both phases. However, a spin switch cannot be discarded for Ag_{25} glasses.

Acknowledgements

The authors are grateful to: Dr. M.F. Van Raap for her friendly collaboration with low temperature Mössbauer measurements. Technological Research Centre (CINI) Tenaris S.A., Argentina, for Scanning Electron Microscopy. ANPCyT (project PICT03-14383), Universidad de Buenos Aires (project IN023) and CONICET (PIP6146) for their constant support.

References

[1] A. Prince, in: G. Petzow, G. Effenberg (Eds.), Ternary Alloys, VCH, New York, 1988, p. 195.
[2] A. Piarristeguy, M. Mirandou, M. Fontana, B. Arcondo, J. Non-Cryst. Solids 273 (2000) 30.
[3] M.A. Ureña, M. Fontana, B. Arcondo, M.T. Clavaguera-Mora, J. Non-Cryst. Solids 320 (2003) 151.
[4] M.A. Ureña, A. Piarristeguy, M. Fontana, B. Arcondo, Solid State Ionics 176 (2005) 505.
[5] B. Arcondo, M.A. Ureña, A. Piarristeguy, A. Pradel, M. Fontana, Physica B 389 (2007) 77.
[6] A. Piarristeguy, M. Ramonda, A. Ureña, A. Pradel, M. Ribes, J. Non-Cryst. Solids 353 (2007) 1261.
[7] J. Kawamura, N. Kuwata, K. Hattori, J. Mizusaki, Rep. Inst. Fluid Sci. 19 (2007) 67.
[8] J.W. Cahn, J. Chem. Phys. 42 (1965) 93.
[9] B. Arcondo, M.A. Ureña, J.M. Conde Garrido, J.A. Rocca, M. Fontana. Int. Conf. on the Appl. of the Mössbauer Effect 2009 Proc., J. Phys.: Conf. Ser., in press.
[10] M. Mitkova, Yu Wang, P. Boolchand, Phys. Rev. Lett. 83 (1999) 3848.
[11] Y. Wang, M. Mitkova, D.G. Georgiev, S. Mamedov, P. Boolchand, J. Phys. Condens. Matter 15 (2003) S1573.
[12] A.A. Piarristeguy, G.J. Cuello, B. Arcondo, A. Pradel, M. Ribes, J. Non-Cryst. Solids 353 (2007) 1243.
[13] A.A. Piarristeguy, G.J. Cuello, P. Yot, A. Pradel, M. Ribes, J. Phys. Condens. Matter 20 (2008) 155106.
[14] T. Abe, M. Shimono, K. Hashimoto, K. Hono, H. Onodera, Scripta Mater. 55 (2006) 421.
[15] A. Piarristeguy, J.M. Conde Garrido, M.A. Ureña, M. Fontana, B. Arcondo, J. Non-Cryst. Solids 353 (2007) 3314.
[16] M. Kawasaki, J. Kawamura, Y. Nakamura, M. Aniya, Solid State Ionics 123 (1999) 259.
[17] A. Pradel, N. Kuwata, M. Ribes, J. Phys. Condens. Matter 15 (2003) S1561.
[18] V. Balan, A. Piarristeguy, M. Ramonda, A. Pradel, M. Ribes, J. Optoelectr. Adv. Mater. 8 (2006) 2112.
[19] B Arcondo, M.A. Ureña, M. Erazú, J.A. Rocca, M. Fontana, Hyperfine Interact. 182 (2008) 137.